PAPER

Check for updates

Transtympanic delivery of V$_2$O$_5$ nanowires with a tympanic-membrane penetrating peptide†

Sophie S. Liu,[a,b] Jiayan Lang, [ID][a] Shuxian Wen, [ID][a] Pengyu Chen,[a] Haonian Shu,[a] Simon Shindler, [ID][a] Wenjing Tang, [ID][a] Xiaojing Ma, [ID][a] Max D. Serota[a] and Rong Yang [ID] *[a]

Otitis media is a prevalent pediatric condition. Local delivery of antimicrobial agents to treat otitis media is hindered by the low permeability of the stratum corneum layer in the tympanic membrane. While nanozymes, often inorganic nanoparticles, have been developed to cure otitis media in an antibiotic-free manner in a chinchilla animal model, the tympanic membrane creates an impenetrable barrier that prevents the local and non-invasive delivery of nanozymes. Here, we use a newly developed vanadium pentoxide (V$_2$O$_5$) nanowire as an example, which catalyzes the metabolic products of an otitis media pathogen (*Streptococcus pneumoniae*) into antiseptics, to explore the transtympanic delivery strategies for antimicrobial nanozymes. V$_2$O$_5$ nanowires with smaller dimensions (<300 nm in length) were synthesized by optimizing the synthesis conditions. To enhance penetrations across intact tympanic membranes, the nanowire was mixed or surface-modified with a trans-tympanic peptide, TMT3. The peptide-modified nanowires were characterized for their physical properties, catalytic activities, and antimicrobial activities. The cytotoxicity profile and permeation across *ex vivo* tympanic membrane samples were analyzed for the mixed and surface-modified nanozyme formulations.

Introduction

Otitis media (OM) is the most common pediatric infection and is estimated to affect 709 million people globally every year.[1] More than 80% of children in the U.S. will experience at least one episode of otitis media before the age of three,[2] while recurrent episodes (>6) of OM could eventually affect 40% of children.[3] The current standard of care usually consists of a seven to ten-day oral antibiotics course; unfortunately, the frequent use of these broad-spectrum antibiotics due to multiple recurrent episodes of otitis media, paired with a 10% non-compliance rate in the patient finishing the prescription,[4] risks the development of antimicrobial resistance in otitis media pathogens.[5,6]

Previously, we have developed vanadium pentoxide (V$_2$O$_5$) nanowires as a novel antimicrobial agent to combat OM infection caused by *Streptococcus pneumoniae* (*S. pneumoniae*).[7] The V$_2$O$_5$ nanowires belong to a class of haloperoxidase nanozyme that could catalyze the production of hypobromous acid

(HOBr) from bromide ions (Br$^-$) and hydrogen peroxide (H$_2$O$_2$), the latter a metabolic product of *Streptococcus pneumoniae*.[8] Hypobromous acid shares similar reactivities against bacterial membranes with hypochlorous acid (bleach).[9] Unlike other antibiotics, hypobromous acid has reported little antimicrobial resistance, albeit its long history of use in water disinfection, due to its rapid killing of bacteria that occurs within seconds to minutes upon contact.[10]

In the previous work, V$_2$O$_5$ nanowires demonstrated excellent therapeutic efficacy in treating *S. pneumoniae*-induced OM infection in a chinchilla model.[7] However, due to their sub-micron dimensions, the nanowires were not suitable for non-invasive administration but were instead directly administered into the middle ear through a trans-tympanic injection. Non-invasive delivery to the middle ear remains a critical challenge in OM treatment due to the biological barrier – the tympanic membrane – that separates the outer ear and the middle ear.[11] The tympanic membrane is structurally similar to the skin and is likewise known for its exceptionally low permeability. The outermost layer of the tympanic membrane is the stratum corneum, a network of keratin-filled corneocytes embedded in an extracellular lipid matrix that is reported to only allow the penetration of drugs smaller than 500 Da.[12,13] Hence, V$_2$O$_5$ nanowires with an average length ~1000 nm remain practically inaccessible for non-invasive treatments to the middle ear.

[a]*Smith School of Chemical and Biomolecular Engineering, Cornell University, Ithaca, NY, 14850, USA. E-mail: ryang@cornell.edu*

[b]*Meinig School of Biomedical Engineering, Cornell University, Ithaca, NY, 14850, USA*

Although several physical techniques, *e.g.*, electroporation, phonophoresis and iontophoresis, have been explored to temporarily disrupt the stratum corneum in skin, these strategies are less desirable for middle ear delivery given their potential damage to the auditory system.[14] Meanwhile, biological enhancers, such as cell penetrating peptides constructed out of short amino acid sequences (<30 residues), have been frequently used to transport a variety of cargoes, ranging from small molecules to proteins, nanoparticles, and liposomes across lipid membranes.[15,16] These peptide-based permeation enhancers are usually biocompatible and induce little cytotoxicity.[15,16]
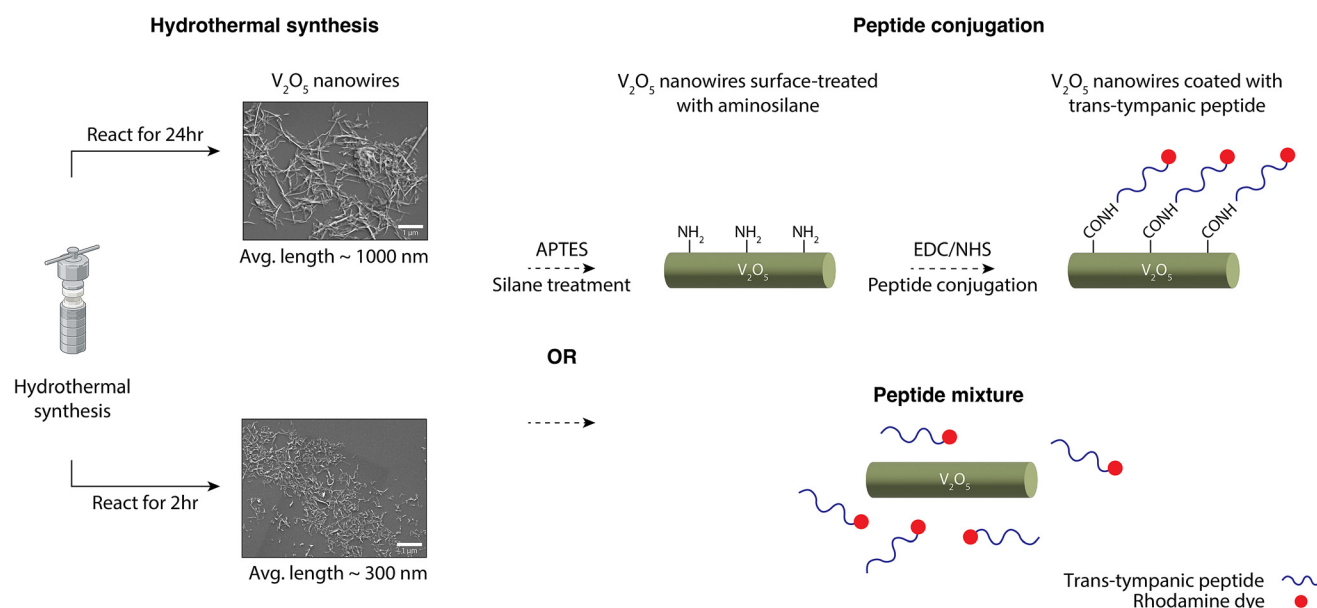
In this work, we demonstrated a strategy to enable the non-invasive delivery of V_2O_5 nanowires into the middle ear, by conjugating a trans-tympanic peptide onto the V_2O_5 nanowire surface to enable transport across the tympanic membrane. The peptide chosen here is TMT3 – an 18-mer peptide that was screened and optimized for transport across infected rat tympanic membrane through phage display.[17–19] Considering the rigidity and the elongated rod-like shape of the V_2O_5 nanowires, we also reduced the dimensions of the nanowires through tuning its synthesis conditions. Hence, the overall workflow for nanowire modification consisted of two modules, as shown in Scheme 1. First, the dimensions of V_2O_5 nanowires were reduced by tuning the synthesis conditions, *e.g.*, reactant ratio, pH, addition of surfactants, and reaction time (ESI Table 1†). Reducing the reaction time proved to be the most effective practice for lowering nanowire dimensions compared to tuning other variables. In the second module, the

nanowires underwent one of the two treatments: simple mixing with the TMT3 peptide or surface-modification with TMT3 peptide for the peptides to be covalently tethered. In the latter case, the nanowires were first treated with an aminosilane, (3-aminopropyl)triethoxysilane (APTES), to introduce amine groups onto nanowire surfaces. These amine groups were then used to react with the free acid (*e.g.*, on the C-terminal) in the TMT3 peptide through (1-ethyl-3-(3-dimethylaminopropyl) carbodiimide/*N*-hydroxysuccinimide) (EDC/NHS) coupling. The N-terminal of the TMT3 peptide was modified with a fluorescent dye, rhodamine. After characterizing their physical properties, we confirmed the catalytic activities of these mixed nanowire formulations or surface-modified nanowires, characterized their antimicrobial efficacies *in vitro*, and assessed their tympanic membrane penetration activities *ex vivo*.

Results and discussion

Synthesis of sub-micron V_2O_5 nanowires

To reduce the size of nanowires, we first looked at changing the parameters for the synthesis process. The reported V_2O_5 nanowires [NW-24 h] were prepared using an established hydrothermal synthesis method (ESI Fig. 1†), with a 24-hour reaction in an autoclave kept at 180 °C containing 8 mmol of $VOSO_4 \cdot nH_2O$, 2.5 mmol of $KBrO_3$ and 15 mL water.[20] Changes were made to various parameters in this protocol, including the reactant ratio, pH, addition of surfactants, and reaction

Scheme 1 An illustration showing the overall workflow of the hydrothermal synthesis of V_2O_5 nanowires followed by mixing with peptide or peptide conjugation. During the hydrothermal synthesis step, the autoclave reaction time is tuned to regulate the average (avg.) length of the nanowires produced. The resulting nanowires are surface-modified with the TMT3 trans-tympanic peptide or mixed with the peptide. During the peptide conjugation step, the nanowires were first treated with (3-aminopropyl)triethoxysilane (APTES) to introduce amino groups onto the surface of nanowires, and then reacted with TMT3 peptide tagged with a rhodamine dye using 1-ethyl-3-(3-dimethylaminopropyl) carbodiimide (EDC) and *N*-hydroxysuccinimide (NHS) chemistry. Illustration partially generated with Biorender.
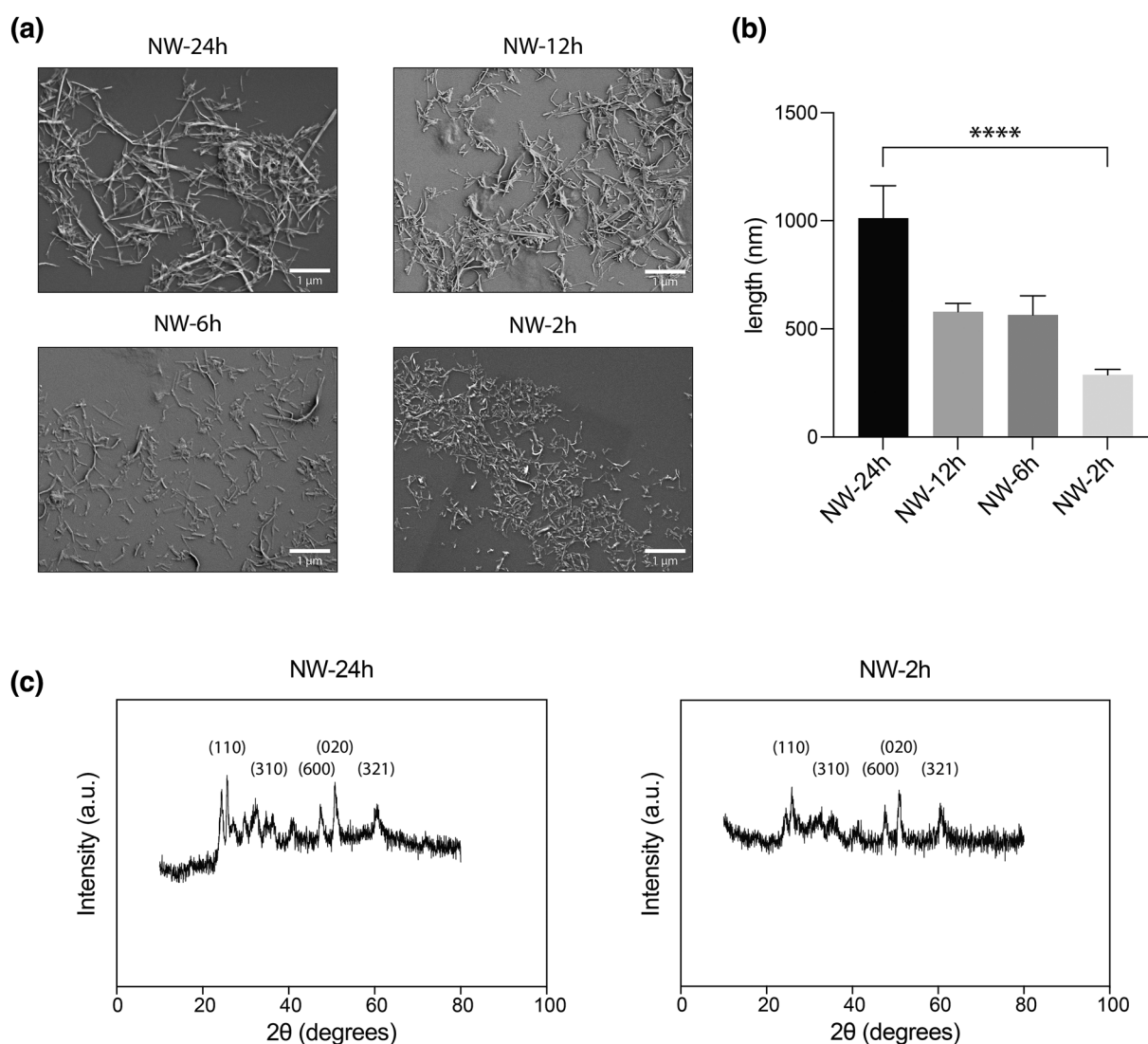
time (ESI Table 1†). The resulting nanowires were characterized through scanning electron microscopy (SEM) for characterization of their lengths.

Of these variables, reducing the reaction time prove to have single-handedly reduced the length of nanowires. Compared to NW-24 h which had an average length of 1012 ± 149 nm (mean ± standard error mean), nanowires that were reacted for 12 hours [NW-12 h], or 6 hours [NW-6 h], or 2 hours [NW-2 h] in the autoclave had average lengths of 579 ± 39 nm, 565 ± 89 nm, and 287 ± 25 nm (Fig. 1a and b). A higher resolution image for Fig. 1a is provided in ESI Fig. 2.† Even though the dimension of NW-2 h has been reduced by more than 3-fold compared to NW-24 h, it exhibited a similar crystalline structure, as shown by the powder X-ray diffraction (XRD) patterns (Fig. 1c). Meanwhile, modulating other parameters of the synthesis method, including the addition of surfactants to reactant mixtures, did not result in notable decreases in the nanowire length (ESI Table 1†).

It should be noted that, V_2O_5 nanocrystals could also be produced from many other methods, including sol–gel, chemical vapor deposition, and atomic layer deposition.[21] The resulting nanocrystals can undertake various morphologies, ranging from 1 dimensional (1D) structures such as nanowires and nanotubes, to 2D nanosheets and 3D frameworks.[21] In this study, hydrothermal synthesis was focused on because it favors the production of 1D nanostructures[22] and as of now, detailed study on the haloperoxidase-like activity of V_2O_5 nanostructures, which can be harnessed to combat otitis media pathogens, have primarily been reported in 1D V_2O_5 structures with defined orthorhombic lattice structures.[20,23] In the

Fig. 1 Changing the reaction time to yield nanowires of different lengths. (a) Representative scanning electron microscopy (SEM) images showing the morphology of nanowires synthesized with 24-hour reaction (NW-24 h), 12-hour reaction (NW-12 h), 6-hour reaction (NW-6 h), or 2-hour reaction (NW-2 h). (b) The lengths of nanowires, measured from the images in (a), shown in mean ± standard error mean, n > 10. (c) Powder X-ray diffraction (XRD) patterns suggest similar crystalline structures between NW-24 h and NW-2 h.

future, it would certainly be of interest to test if other V_2O_5 nanostructures, such as nanoparticles[24,25] and microspheres,[26] could also possess antimicrobial activities.

Peptide mixing or surface-conjugation to the nanowires

For subsequent experiments, [NW-24 h], which has similar dimensions as previously reported nanowires, and [NW-2 h], which possesses lower length profiles, were chosen as the candidates for trans-tympanic permeation studies after peptide modification. The transtympanic peptide, TMT3, was identified through a series of phage display and chosen based on its enhanced ability to permeate *ex vivo* tympanic membrane samples retrieved from rats, guinea pigs, rabbits, and human, as reported in several papers.[17–19] Although the exact mechanism behind TMT3's transtympanic permeation is not fully understood, it is postulated that TMT3 can facilitate macropinocytosis to enable the transcytosis of phages.[27] The peptide forms a primarily linear structure, expressing on one end a STKT motif that is conserved among other transtympanic peptides and even a few protein motifs involved in transmembrane transport.[27]

In the two formulations, [NW-24 h + TMT3] and [NW-2 h + TMT3], free TMT3 peptides were combined with the nanowires through simple mixing and no chemical linkage. Alternatively, the nanowires were surface modified with TMT3 to produce [NW-24 h-TMT3] and [NW-2 h-TMT3] through coupling reactions. The TMT3 peptide used in this study was conjugated with a rhodamine dye on the N-terminal while its C-terminal had a free acid available for crosslinking using the EDC/NHS coupling, which is a method commonly used for linking biomacromolecules with a free amine group.[28] To introduce amine groups onto the nanowire surface, [NW-24 h] and [NW-2 h] were first incubated with APTES, an aminosilane, to produce [NW-24 h-APTES] and [NW-2 h-APTES] (Scheme 1). APTES can undergo hydrolysis with the naturally occurring hydroxyl groups on V_2O_5 nanowire surface to replace the ethoxy group from APTES with a silanol group connected to the nanowire. The secondary amine group from APTES will then be used to react with the carboxylic acid group in the TMT3 peptide *via* EDC/NHS coupling (Scheme 1) to form an amide linkage (Scheme 1), producing [NW-24-TMT3] and [NW-2 h-TMT3].

Successful TMT3 conjugation was first confirmed by X-ray photoelectron spectroscopy (XPS) performed on [NW-2 h], [NW-2 h-APTES], and [NW-2 h-TMT3]. High-resolution XPS scan on N (1s) showed the appearance of two peaks after APTES coating, which may be attributed to the amine group (399.8 eV) and protonated amine group (402.1 eV) from APTES[29,30] (Fig. 2a). After peptide coating, NW-2 h-TMT3 displayed a broad N (1s) peak, which may be deconvoluted into a prominent amide peak (399.6 eV), and two smaller peaks corresponding to free amines (399.2 eV) and protonated amines (401.6 eV), possibly from amino acids in the peptide[31] (Fig. 2a). High-resolution XPS scans on O (1s) and V (2p) also revealed corresponding changes to O 1s peaks after APTES and TMT3 coating while the oxidation states for vanadium ions

remained little changed before and after coatings (Fig. 2a). Similar XPS peak profiles were observed for [NW-24 h], [NW-24 h-APTES], and [NW-24 h-TMT3], confirming the successful APTES coating and TMT3 conjugation on the nanowire surface (ESI Fig. 3†).

Next, confocal microscopy was used as an additional confirmation. Since the N-terminal of TMT3 peptide carried a rhodamine dye, the as-synthesized [NW-2 h-TMT3] nanowires also displayed fluorescent signals that were detected from clusters of surface-modified nanowires that were large enough to be visible under confocal microscopy (Fig. 2b). The fluorescent signals were unlikely to be from aggregates of TMT3 because this peptide is unlikely to form large aggregates with itself, due to its predicted unstructured β-chain configuration.[27]

Fourier-transform infrared spectroscopy (FTIR) also confirmed the APTES and TMT3 coating on [NW-24 h] and [NW-2 h] nanowires. The FTIR spectra for [NW-24 h-APTES] and [NW-2 h-APTES] showed the characteristic peak at 1100 cm^{-1} corresponding to Si–O–Si and the peak at 1500 cm^{-1} corresponding to NH_2 group[32] (ESI Fig. 4†). The FTIR spectra for [NW-24 h-TMT3] and [NW-2 h-TMT3] both showed a broad band in the amide I region,[33,34] around 1600–1700 cm^{-1}, but this region overlaps with the hydroxyl peak from the uncoated V_2O_5 surface,[35] making peaks hard to distinguish, meanwhile a peak at 1280 cm^{-1} corresponding to the amide III region[33,34] could be identified, confirming the presence of peptide structures on the surface of TMT3-coated nanowires (ESI Fig. 4†).
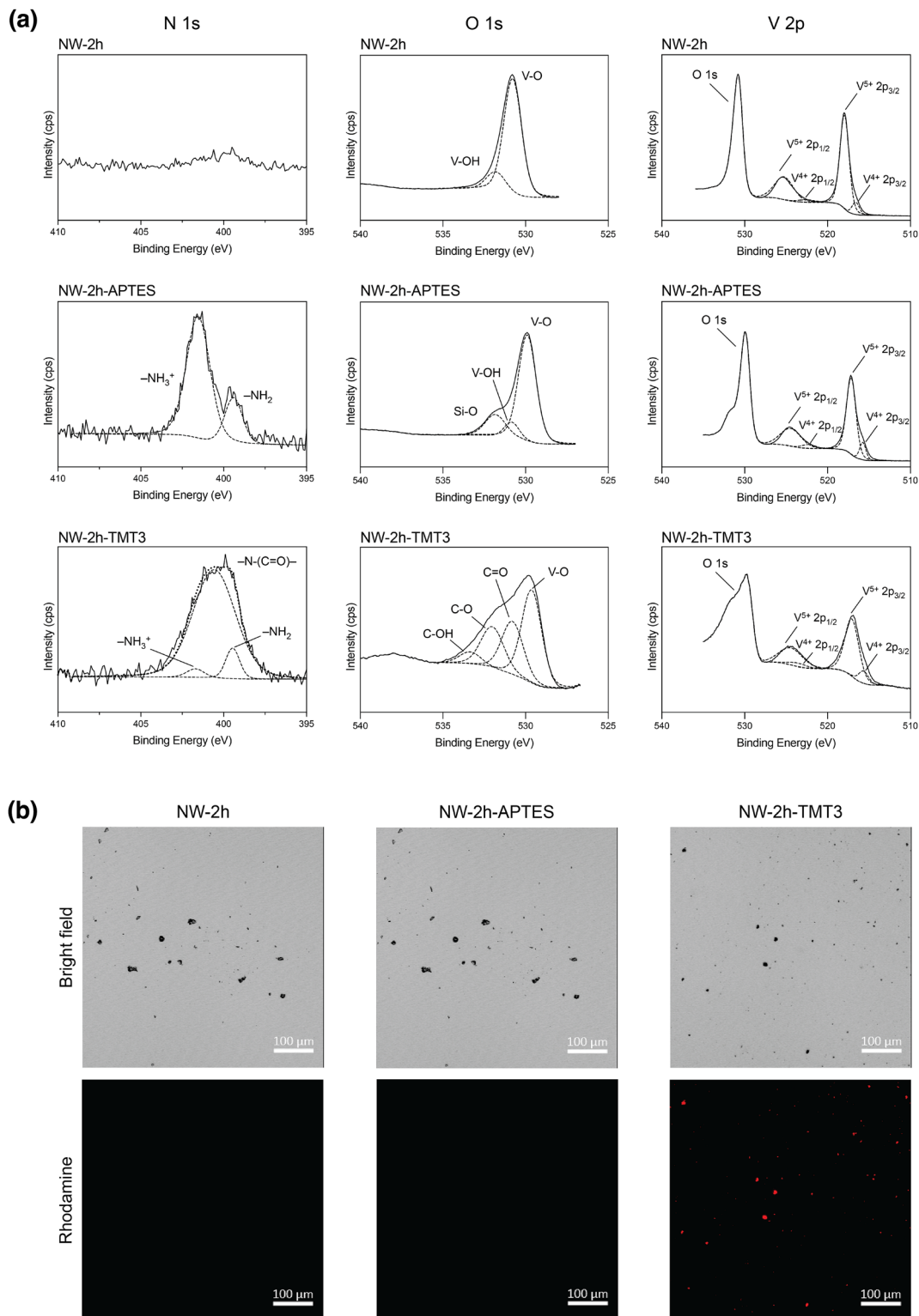
Catalytic activity

Next, the nanowires were investigated for their catalytic activity, which is the basis for their antimicrobial effect, before and after surface modifications. The V_2O_5 nanowires derive their haloperoxidase-like catalytic efficacy from a specific vanadium coordination geometry embedded in the lattice structures,[20] and the nanowires can thus catalyze the production of HOBr from Br^- ions and H_2O_2. The generated HOBr can eradicate micro-organisms in a fashion similar to hypochlorous acid (bleach) and breed little antimicrobial resistance.[10]

The phenol red (PR) assay was used to test for HOBr generation catalyzed by the nanowires, in an aqueous solution containing 0.04 mg mL^{-1} nanowires, 100 mM Br^- ions, 5 mM H_2O_2, and 50 μM PR molecules. After HOBr is generated, it can induce the bromination of PR to bromophenol blue (Br_4PR), causing an increase in the absorbance of Br_4PR that can be captured by visible light spectroscopy (Fig. 3a and b). As a measure of the catalytic activity of nanowires, the initial rate of the production of Br_4PR (v_0), which can be assumed to be the rate of HOBr generation, was calculated based on the change in its absorbance reading over 10 minutes at 37 °C, using the Lambert–Beer law (see Method for details).

Both [NW-24 h] ($v_0 = 6.21 \times 10^{-9} \pm 1.13 \times 10^{-9}$ μM min^{-1}, mean ± standard deviation, SD) and [NW-2 h] possessed a
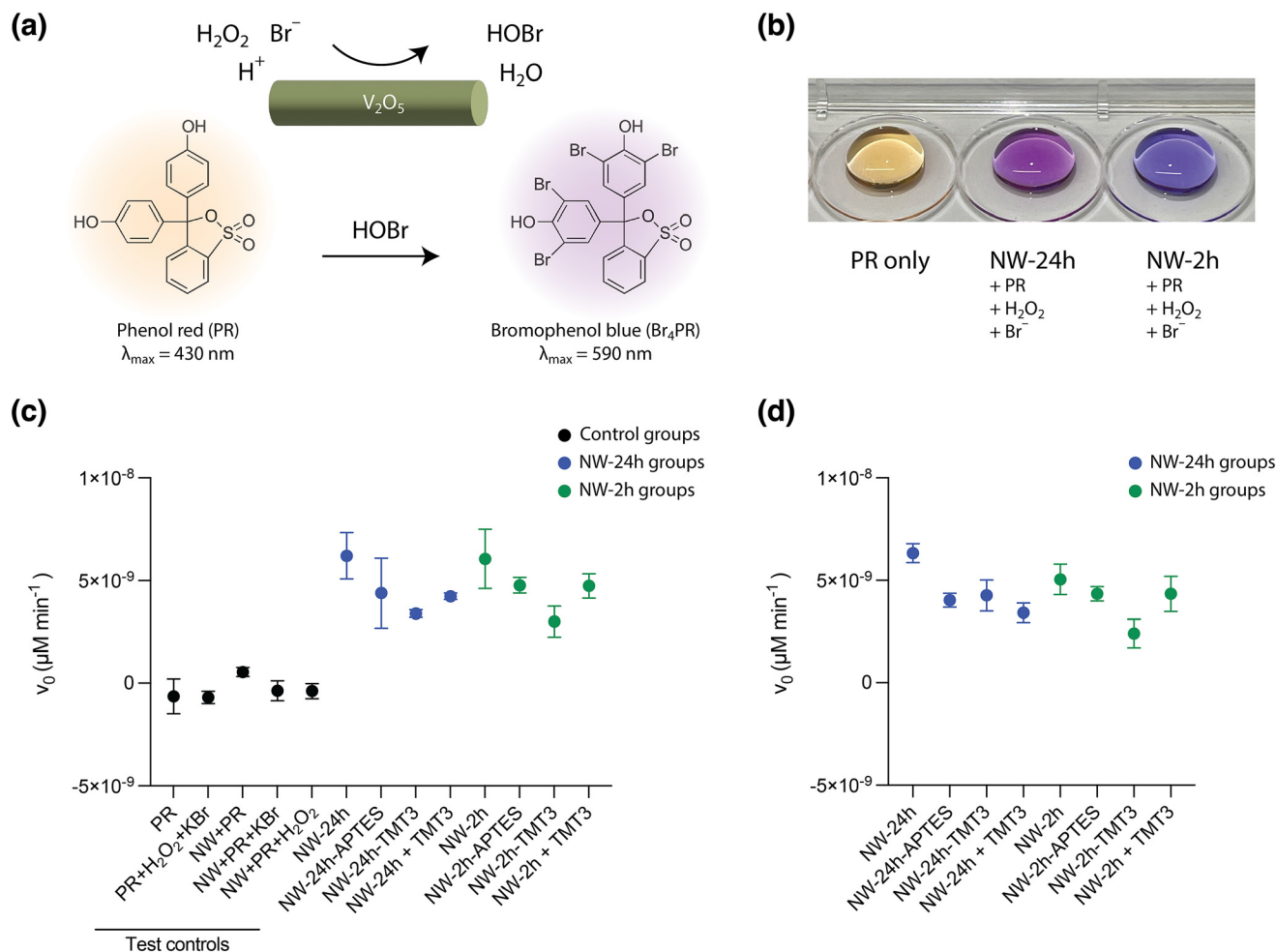
Fig. 2 Surface modification of NW-2 h with trans-tympanic peptides. (a) High-resolution X-ray photoelectron spectroscopy (XPS) scan on N (1s), O (1s), and V (2p) showing changes to the surface binding energy on NW-2 h before and after APTES and TMT3 coating. (b) Representative confocal microscopy images showing large clusters of NW-2 h, NW-2 h-APTES and NW-2 h-TMT3; fluorescent signals from the rhodamine tag on TMT3 was only witnessed from NW-2 h-TMT3.

Fig. 3 Phenol red (PR) assay to measure the catalytic activity of V_2O_5 nanowires. (a) An illustration showing the bromination reaction used to quantify the reaction kinetics of HOBr generation catalyzed by V_2O_5 nanowires. (b) A photograph showing the color change for 50 μM PR after 24 hours of incubation with 0.04 mg mL^{-1} NW-24 h or NW-2 h, 5 mM H_2O_2 and 100 mM KBr in 0.5× PBS solution. (c) The rate of reactions of the bromination assay for nanowires before and after surface coating (n = 3−6); the ingredients of the reaction mixture for "Test controls" are indicated on the x-axis labels, whereas the experimental groups all contained 0.04 mg mL^{-1} nanowire, 50 μM PR, 5 mM H_2O_2 and 100 mM KBr in 0.5× PBS solution; the test controls contained at least one less element of the reaction mixture listed above, at the same concentration, and NW-2 h was used for control groups. (d) The rate of reactions of the bromination assay for nanowires measured after 24 hours of incubation in the reaction mixture (n = 3−6).

similar catalytic activity (v_0 = 6.01 × 10^{-9} ± 1.44 × 10^{-9} μM min^{-1}) (Fig. 3c), corroborating the previous XRD analysis that reducing the reaction time of V_2O_5 nanowires to 2 hours did not affect its unique crystalline structure nor its haloperoxidase-like nanozyme activity. After APTES and TMT3 coating, the initial bromination rates for [NW-24 h-APTES], [NW-24-TMT3], [NW-2 h-APTES], and [NW-2 h-TMT3] shifted to 4.39 × 10^{-9} ± 1.90 × 10^{-9} μM min^{-1}, 3.39 × 10^{-9} ± 1.85 × 10^{-10} μM min^{-1}, 4.77 × 10^{-9} ± 3.80 × 10^{-10} μM min^{-1} and 3.01 × 10^{-9} ± 7.56 × 10^{-10} μM min^{-1}, respectively (Fig. 3c). When the bare nanowires were mixed with free TMT3 peptides, the initial bromination rates for [NW-24 h + TMT3] and [NW-2 h + TMT3] were 4.23 × 10^{-9} ± 1.55 × 10^{-10} μM min^{-1} and 4.74 × 10^{-9} ± 5.94 × 10^{-10} μM min^{-1}, respectively (Fig. 3c).

After remaining in the reaction mixture for 24 hours, the nanowires still retained their catalytic activities. The bromination kinetics for [NW-24 h], [NW-24 h-APTES], [NW-24 h-TMT3], [NW-24 h + TMT3], [NW-2 h], [NW-2 h-APTES], [NW-2 h-TMT3], and [NW-2 h + TMT3] were measured to be 6.33 × 10^{-9} ± 7.94 × 10^{-10} μM min^{-1}, 4.03 × 10^{-9} ± 3.38 × 10^{-10} μM min^{-1}, 4.26 × 10^{-9} ± 7.60 × 10^{-10} μM min^{-1}, 3.42 × 10^{-9} ± 1.17 × 10^{-9} μM min^{-1}, 5.05 × 10^{-9} ± 1.29 × 10^{-10} μM min^{-1}, 4.35 × 10^{-9} ± 3.48 × 10^{-10} μM min^{-1}, and 2.41 × 10^{-9} ± 6.96 × 10^{-10} μM min^{-1}, 4.34 × 10^{-9} ± 2.10 × 10^{-9} μM min^{-1}, respectively (Fig. 3d).
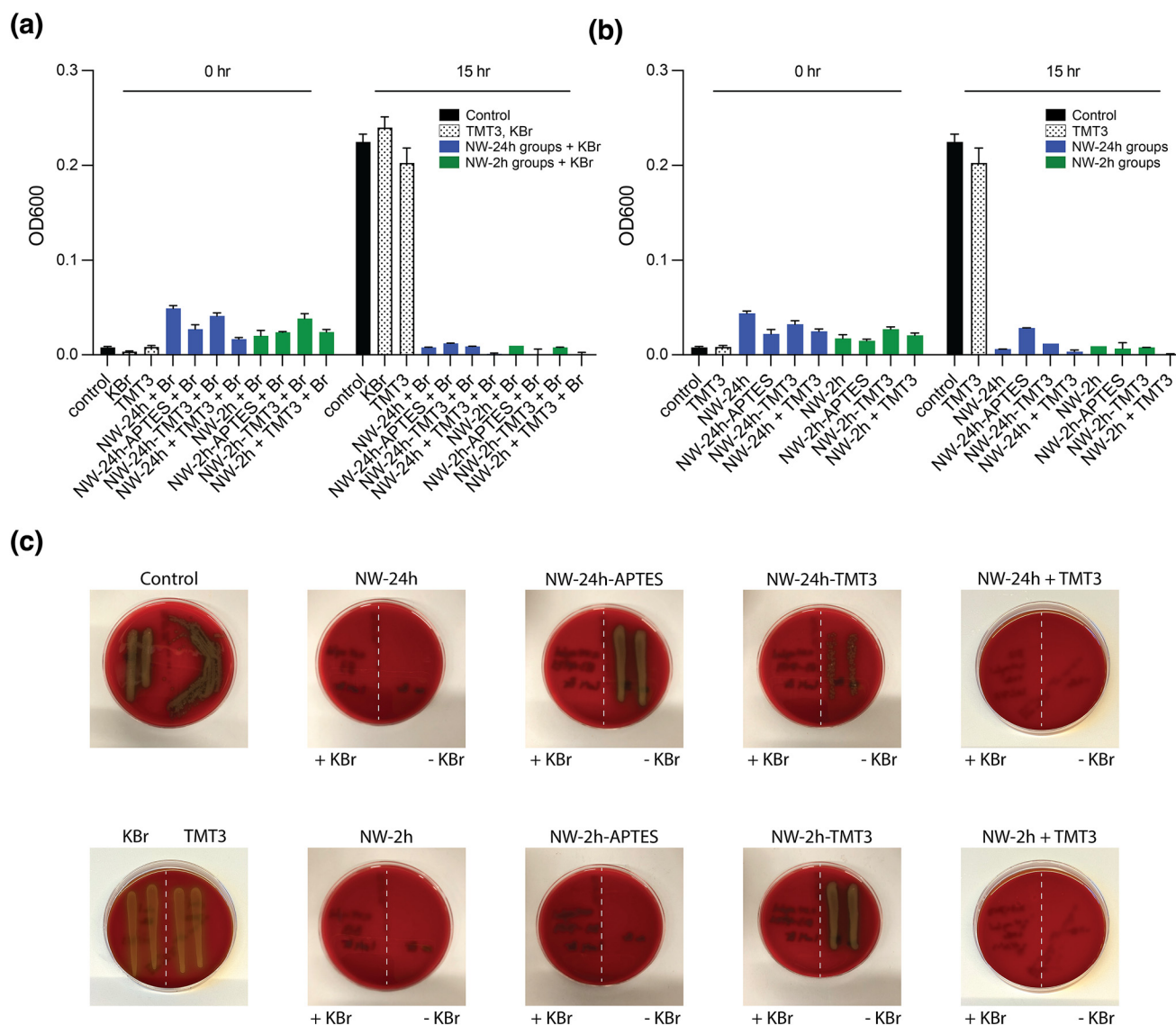
Antimicrobial study

To assess the antimicrobial activity of the nanowires after mixing with the peptide or the peptide conjugation, an *in vitro* assay was performed using a clinically isolated strain of *S. pneumoniae* which is a common OM pathogen. *S. pneumoniae* is known to secrete H_2O_2 as a metabolic product, and the concentration of H_2O_2 in liquid broth can reach ~1 mM after overnight culture.[8] Although [NW-2 h] and [NW-24 h] were produced under different reaction time, they

possessed similar antimicrobial efficacy against *S. pneumoniae* upon the addition of Br⁻ ions (ESI Fig. 5a†), corroborating with the catalytic activity study where similar bromination kinetics were witnessed between these two uncoated nanowire groups.

Next, the antimicrobial activities of unmodified, peptide-mixed and surface modified-nanowires were tested in a mixture that contained 0.04 mg mL⁻¹ nanowires and 1 mM KBr (as the source of Br⁻ ions) added to *S. pneumoniae* subculture in liquid broth. After 15 hours of incubation, the stationary phase optical density at 600 nm (OD600) was measured, and a clear suppression of *S. pneumoniae* growth was achieved for [NW-2 h] and [NW-24 h] (Fig. 4a). Similar results were

obtained after surface coating for [NW-2 h-APTES] and [NW-2 h-TMT3], [NW-24 h-APTES] and [NW-24 h-TMT3]. Although the PR assay has indicated reduced catalytic activities for nanowires after APTES and TMT3 coating, their antimicrobial efficacies against *S. pneumoniae* growth were still comparable to uncoated nanowires, according to the antimicrobial assay (Fig. 4a). Furthermore, similar antimicrobial activities were observed for nanowires mixed with free peptide, [NW-24 h + TMT3] and [NW-2 h + TMT3] (Fig. 4a), indicating the addition of the free peptide did not interfere with the nanowire's catalytic reactions. A separate dilution assay also confirmed that the TMT3 peptide itself is not antimicrobial (ESI Fig. 5b†).

Fig. 4 Antimicrobial effects of the nanowires against *S. pneumoniae*. (a) Optical density at 600 nm (OD600) readings of *S. pneumoniae* cultures treated with 0.04 mg mL⁻¹ nanowires and 1 mM KBr, before (0 h) and after (15 h) 15 hours of incubation (*n* = 3). (b) OD600 readings of *S. pneumoniae* cultures treated with 0.04 mg mL⁻¹ nanowires only, before (0 h) and after (15 h) 15 hours of incubation (*n* = 3). (c) Images of blood agar plates that were plated with aliquots of the *S. pneumoniae* cultures at the end of the 15-hour incubation from (a) and (b); except for the control, KBr, and TMT3 group, the left half of the plate contained aliquots from bacteria cultures from (a) that were treated with nanowires and KBr, and the right half of the plate contained aliquots from (b) that were treated with nanowires but without KBr.

Interestingly, when nanowires alone were added to the bacteria subculture (without supplementing Br^- ions to aid the production of HOBr), a similar growth suppression was witnessed from OD600 reading (Fig. 4b). However, since OD600 may not completely reflect bacteria viability, aliquots of the liquid broth (10 µl) were taken after OD600 measurement and immediately plated onto blood agar plates for overnight culture as a confirmation measure. As seen from the agar plates, only when both nanowires and KBr were added for [NW-24 h-APTES], [NW-24 h-TMT3], and [NW-2 h-TMT3], were the bacteria fully eradicated (Fig. 4c). This corroborates the previous observation of a partial reduction in bacterial growth after nanowire treatments without Br^- ions.[7] This may have been caused by the small amount of Br^- ions (~38 µM) present in the liquid media used for bacteria culture, supplemented BHI (suppBHI, see Method for details) (ESI Fig. 6a†). When suppBHI was diluted into the PR bromination reactant mixture (0.04 mg mL^{-1} NW-24 h, 50 µM PR, 5 mM H_2O_2 and ~25% suppBHI), measurable catalytic activity was witnessed even without KBr supplement, suggesting that the Br^- ions from bacteria culture media can support small levels of HOBr generation (ESI Fig. 6b†). However, Br^- ions should be supplemented whenever possible to ensure full antimicrobial effect.

Cytotoxicity study

The cytotoxicity of the nanowires was tested using human fibroblast cells (hFB) and PC12 (a pheochromocytoma cell line used for ototoxicity testing). Cells were incubated for 24 hours with either 0.01 mg mL^{-1} or 0.04 mg mL^{-1} of nanowires ([NW-24 h], [NW-24 h-APTES], [NW-24 h-TMT3], [NW-24 h + TMT3], [NW-2 h], [NW-2 h-APTES], [NW-2 h-TMT3], [NW-2 h + TMT3]), and supplemented with 1 mM Br^- (from KBr solution) and 10 µM H_2O_2, according to the experimental settings in a previously reported study.[7] Afterwards, cell proliferation was assessed through the CCK8/WST-8 kit. The addition of low concentration (0.01 mg mL^{-1}) of nanowires caused an inhibition on the growth of hFB cells to 50%–69% compared to untreated control while increasing the nanowire concentration to 0.04 mg mL^{-1} further reduced the growth rates to 26%–46% (Fig. 5a). For PC12 cells, 0.01 mg mL^{-1} of nanowires caused growth rate reductions to 73%–100% while 0.04 mg mL^{-1} of nanowires caused reductions to 31%–48% (Fig. 6a).

To further assess the cytotoxic effects of the nanowires, hFB and PC12 cells were also stained with the Live/Dead kit for visual counting of the percentage of live and dead cells after nanowire treatment. Although 0.01 mg mL^{-1} of nanowires had notably reduced the proliferation of hFB and PC12 cells, they had caused minimal cell deaths as captured by Live/Dead staining, meanwhile 0.04 mg mL^{-1} of nanowires showed mild cytotoxic effects (Fig. 5b, c, 6b, and c). Overall, the nanowires' cytotoxicity is consistent with a previous report[7] and it should be noted that the *in vitro* monolayer cell cultures may be more susceptible to cytotoxic damages than the tissues in the tympanic membrane because the top layer of the tympanic membrane is constructed of the multi-layered stratum corneum, filled with keratin-rich corneocytes and lipid lamellae.[11]

To examine the tissue toxicity against tympanic membranes, healthy chinchillas were treated with 200 µL buffer which contained 0.6 mg NW-2 h-TMT3 and 75 mM Br^- ions through a non-invasive injection to the outer ear canal. After 7 days, the treated tympanic membranes were retrieved for histological analysis where the tympanic membrane was sectioned and stained with haematoxylin and eosin (H&E). Compared to a healthy tympanic membrane (with a thickness of 19.0 ± 4.5 µm, mean ± SD), treatment with NW-2 h-TMT3 did not significantly alter the tympanic membrane's thickness (30.7 ± 19.0 µm) or morphology (ESI Fig. 7†). In terms of potential systemic toxicity, a large proportion of the nanowire formulation is expected be easily removable from the outer ear canal, with a small proportion permeating into the middle ear. Previously, it has been shown that NW-24 h nanowires (0.08 mg) injected directly into the middle ear did not cause noticeable hearing loss over 7 days.[7] It is also possible that small amounts of permeated nanowires may enter systemic circulation, however, this amount will be much lower than the reported LD50 of V_2O_5 which ranges from 10 to 137 mg per kg body weight.[36]
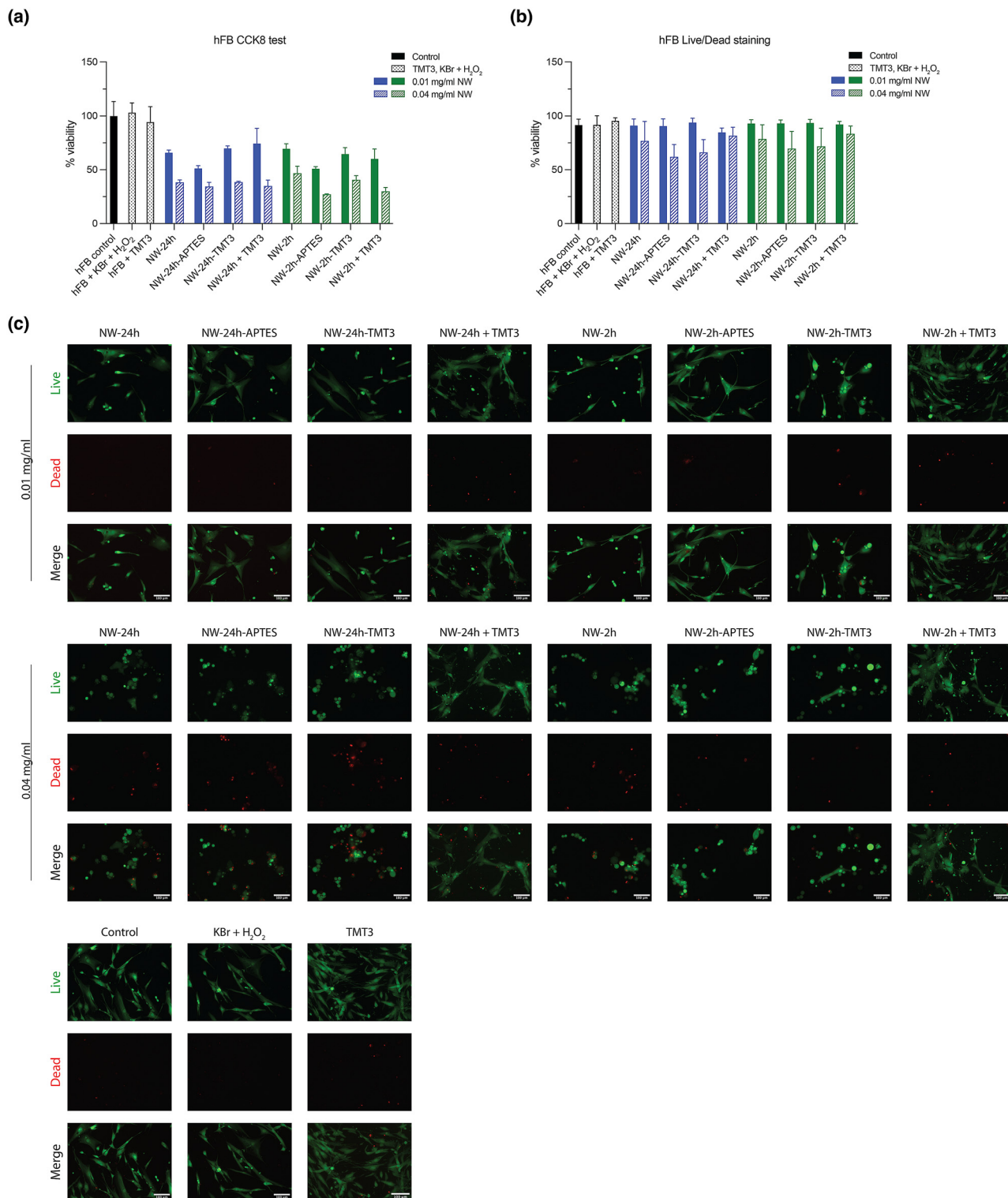
Ex vivo permeation study

To assess the peptide-modified nanowires' transport across intact tympanic membranes, an *ex vivo* permeation study was performed. Chinchilla models were used because their ear anatomy closely approximates that of humans.[37,38] The animals were first inoculated with bacteria to induce inflammation for two days, then the animals were euthanized, and their bullae were retrieved for *ex vivo* permeation study (Fig. 7a). The bullae were excised such that the middle ear chamber was opened and filled with phosphate buffered saline (PBS). The formulations were administered to the outer ear side of the tympanic membrane through the external ear canal. After 48 hours, the study was terminated to avoid complications due to tissue degradation from incubation at 37 °C and the buffer from the middle ear chamber was collected and analyzed with inductively coupled plasma mass spectroscopy (ICP-MS). During this period of time, the nanowires were not expected to disintegrate or experience considerable morphological change, based on the SEM images of the nanowires taken after 120 hours of incubation in PBS at 37 °C (ESI Fig. 8†).

Three experimental groups were compared: 0.6 mg unmodified [NW-24 h] or [NW-2 h], 0.6 mg unmodified NW-24 h or NW-2 h mixed with 50 µM of free TMT3 peptides ([NW-24 h + TMT3] and [NW-2 h + TMT3]), and peptide-modified [NW-24 h-TMT3] or [NW-2 h-TMT3]. All groups were co-administered with 120 µg KBr (75 mM) in 200 µl PBS buffer to the external ear canal. Two additional control groups received 200 µl PBS buffer or 200 µl PBS buffer with 120 µg KBr (Fig. 7).

For the unmodified [NW-24 h], 0.47 ± 0.38% (mean ± SD) of the vanadium contents permeated across the tympanic membrane, meanwhile surface modification with TMT3 peptides slightly increased that percentage to 0.75 ± 0.47% for [NW-24 h-TMT3] (albeit with low statistical significance: p = 0.5816 *vs.* [NW-24 h]) (Fig. 7b). Simply mixing the TMT3 pep-
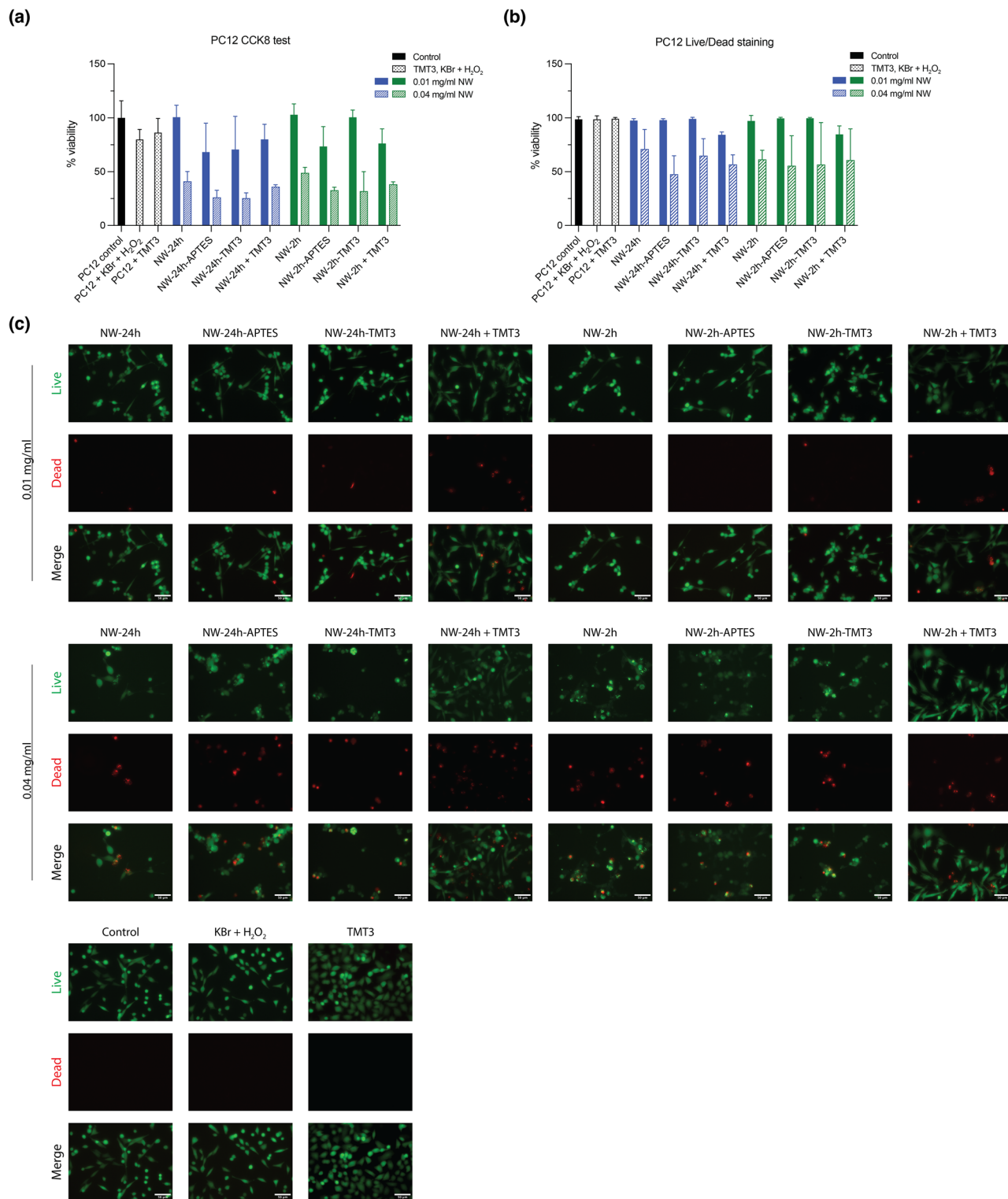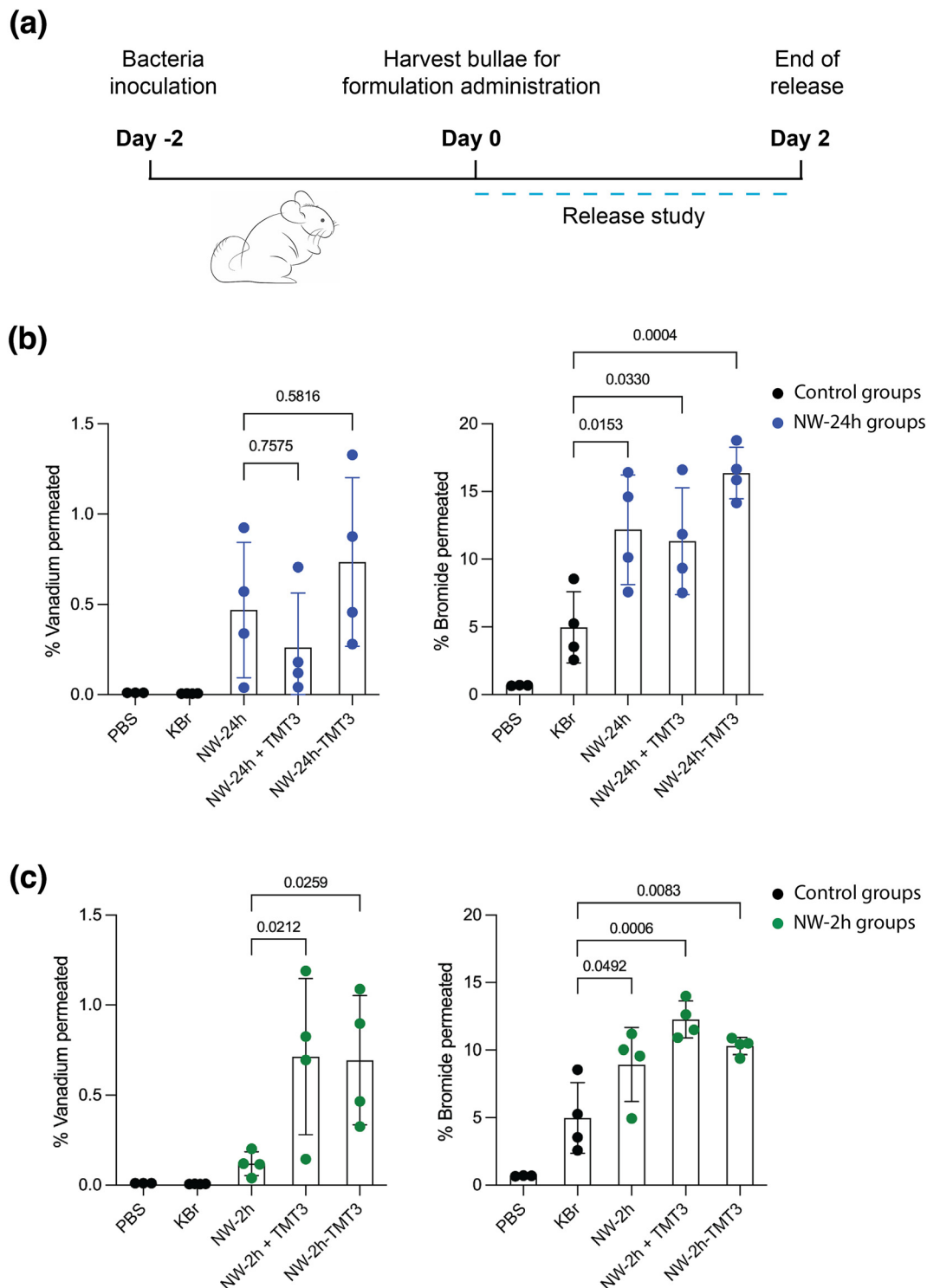
Fig. 5 Nanowire cytotoxicity study with human fibroblast cells (hFB). (a) The viability of human fibroblast (hFB) cells treated with 0.01 mg mL^{-1} or 0.04 mg mL^{-1} nanowires, 1 mM KBr, and 10 μM H_2O_2 for 24 hours, measured using the CCK8 kit (n = 3). (b) The viability of hFB cells after the same treatment as in (a) and measured using immunofluorescent staining (n = 3); live and dead cells were stained with calcein-AM and ethidium homodimer-1, respectively; viability was calculated as (live cells)/(live + dead cells) × 100% (c) Representative images used for calculation in (b), scale bar = 100 μm.

Fig. 6 Nanowire cytotoxicity study with PC12 cells. (a) The viability of PC12 cells treated with 0.01 mg mL^{-1} or 0.04 mg mL^{-1} nanowires, 1 mM KBr, and 10 μM H$_2$O$_2$ for 24 hours, measured using the CCK8 kit ($n = 3$). (b) The viability of PC12 cells after the same treatment as in (a) and measured using immunofluorescent staining ($n = 3$); live and dead cells were stained with calcein-AM and ethidium homodimer-1, respectively; viability was calculated as (live cells)/(live + dead cells) × 100% (c) Representative images used for calculation in (b), scale bar = 50 μm.

Fig. 7   The *ex vivo* permeation study. (a) A scheme showing the *ex vivo* permeation study's timeline. (b) The percentage of vanadium and Br⁻ ions that permeated across the tympanic membrane after 48 hours of incubation with various formulations (n = 3−4). (c) The percentage of vanadium and Br⁻ ions that permeated across the tympanic membrane after 48 hours of incubation with various formulations (n = 3−4). Statistical analysis done using one-way analysis of variance (ANOVA) and Dunnett's multiple comparisons.

tides in [NW-24 h + TMT3] did not increase the percentage of vanadium contents across the tympanic membrane (0.26 ± 0.30%, p = 0.7575 *vs.* [NW-24 h]).

Compared to unmodified [NW-2 h], where 0.12 ± 0.07% of the vanadium contents permeated across the tympanic membrane, the surface modification with TMT3 peptides increased

that percentage for [NW-2 h-TMT3] to 0.69 ± 0.36% (p = 0.0259 vs. [NW-2 h]) (Fig. 7c). The addition of free TMT3 peptides for [NW-2 h + TMT3] also increased that percentage to 0.55 ± 0.36% (p = 0.0212 vs. [NW-2 h]), suggesting that when the nanowires are small enough, addition of free TMT3 peptides may also slightly improve the permeability of the tympanic membrane (Fig. 7c). Unlike the nanowires, the Br^- ions had a much higher permeability, given their small size. In the control group that was treated with 120 µg KBr in 200 µl PBS, 4.98 ± 2.63% of the Br^- ions permeated across the tympanic membrane by 48 hours (Fig. 7b and c). This number was increased to 12.18 ± 4.04%, 11.33 ± 3.95%, and 16.37 ± 1.91% after co-administration with [NW-24 h], [NW-24 h + TMT3], and [NW-24 h-TMT3], respectively (Fig. 7b). The percentage of Br^- ion permeation was also increased to 8.93 ± 2.75%, 12.5 ± 1.5%, and 10.3 ± 0.6% after co-administration with [NW-2 h], [NW-2 h + TMT3], and [NW-2 h-TMT3], respectively (Fig. 7c).

Experimental

Materials

Potassium bromate ($KBrO_3$, 98%), Nitric acid (70%), KBr (99.0%), APTES (≥98%), EDC (≥97%), NHS (98%), and 2-mercaptoethanol (≥99%) was purchased from Sigma-Aldrich (St Louis, MO, USA). Vanadyl sulphate ($VOSO_4 \cdot H_2O$, 99.9% metal basis) and PR was purchased from Thermo Scientific Chemicals (Waltham, MA, USA). H_2O_2 (30% in water) was purchased from Fisher Chemical (Waltham, MA, USA). The 18-mer TMT3 peptide (EGHLFPSADSTKTTHLTL) was ordered from Biomatik (Kitchener, Ontario, Canada) with a free acid on the C-terminal and a rhodamine dye attached to the N-terminal.

Hydrothermal synthesis

V_2O_5 nanowires were synthesized using a previously described hydrothermal method,[7,20] with slight modifications. Briefly, 8 mmol of $VOSO_4 \cdot nH_2O$ and 2.5 mmol of $KBrO_3$ were dissolved in 15 mL distilled water in a round bottom flask and immediately stirred for 15 minutes at room temperature. If the solution's pH was not below 2, nitric acid was added dropwise until pH < 2 was reached. The reactant mixture was then transferred to a Teflon-lined stainless-steel autoclave and the autoclave was placed into an oven heated to 180 °C and allowed to react for 2, 6, 12, or 24 hours. After the pre-determined reaction time, the autoclave was allowed to cool down to room temperature, and the reactant mixture was transferred to a 50 mL conical centrifuge tube and washed with distilled water for 3 times followed by wash with ethanol for 3 times, each time through centrifugation at 6500g for 50 minutes. The precipitate from the last wash was re-suspended in water and dried by lyophilization.

SEM

Nanowires were dispersed in distilled water at 1 mg mL^{-1} and sonicated for >2 hours until homogenous. The 1 mg mL^{-1} nanowire solution was then diluted with 100% ethanol to make 0.1 mg mL^{-1} nanowire and immediately drop-casted onto a clean 1 × 1 cm silicon wafer. The silicon wafer was placed onto a SEM stub with carbon adhesive and the edge of its surface was covered with a piece of conductive copper tape. The SEM images were acquired on a Zeiss Gemini 500 SEM microscope, using a voltage of 1 kV, and captured with the SE-HE2 detector.

XRD

The XRD scans for nanowire samples were collected on a Bruker D8 Advance ECO powder diffractometer. Scans were performed over an angle range from 10° to 80° and collected using a 1 kW Cu-Kα X-ray source.

Nanowire silanization and peptide conjugation

To make APTES-coated nanowires, the nanowires were first dispersed in 100% ethanol at 3 mg mL^{-1} and briefly homogenized with a 10 seconds ON/10 seconds OFF cycle for 5 min on ice or until well-mixed. Then, 2% APTES solution was prepared in pure ethanol and activated at room temperature for 10 minutes. Equal parts of the APTES solution and nanowire solution were mixed and allowed to react for 20 minutes at room temperature. Then the solution was diluted with excess ethanol and centrifuged at 6500g for 50 minutes. The precipitate was washed with 100% ethanol for three cycles and with distilled water for one cycle, and then lyophilized.

To make peptide-coated nanowires, the APTES-coated nanowires were dispersed in water at 1 mg mL^{-1} and briefly homogenized with a 10 seconds ON/10 seconds OFF cycle for 5 min on ice or until well-mixed. The nanowires, TMT3 peptide, EDC, and NHS were all prepared fresh each time. To first make the NHS-ester, TMT3 peptide was dissolved in milliQ water along with 0.4 mg EDC and 0.6 mg NHS per 2 mg peptide. This peptide mixture was adjusted to pH ~ 4.5 using MES buffer and hydrochloric acid, then allowed to react at room temperature away from light for 15 minutes, and quenched with 2-mercaptoethanol. Next, to form the amide linkage, the peptide mixture was combined with the APTES-coated nanowires and the resulting mixture was adjusted to pH ~ 8 using PBS buffer and sodium hydroxide, then allowed to react at room temperature away from light for 2 hours, and quenched with Tris-HCl. The reaction mixture was centrifuged at 6500g for 50 minutes at 10 °C and washed with milliQ water for three cycles, and then lyophilized.

The nanowires were imaged on a Zeiss LSM 710 confocal microscope to confirm the presence or absence of rhodamine fluorescence from the TMT3 peptide. For confocal microscopy, the nanowires were not sonicated so that large nanowire clusters may be visualized.

XPS

Samples were analyzed using a Thermo Scientific Nexsa G2 Spectrometer with operating pressure ca. 1 × 10^{-9} Torr. Monochromatic Al Kα X-rays (1486.6 eV) were generated at 250 W (15 kV; 20 mA) with photoelectrons collected from a 400 µm diameter analysis spot. Photoelectrons were collected at a 90° emission angle with source to analyzer angle of 54.7°. A hemispherical analyzer determined electron kinetic energy, using a

pass energy of 200 eV for wide/survey scans, and 50 eV for high resolution scans. A flood gun was used for charge neutralization of non-conductive samples.

FTIR

FTIR measurements were performed on a Bruker Vertex V80v vacuum FTIR system in attenuated total reflection (ATR) mode. A deuterated triglycine sulfate (DTGS) KBr detector over the range of 600–4000 cm^{-1} was used with a resolution of 4 cm^{-1}. The measurements were averaged over 64 scans to obtain a sufficient signal-to-noise ratio. All the spectra were baseline-corrected by subtracting a background spectrum of bare Si and ATR-corrected.

Phenol red assay

The PR bromination assay was employed to quantify the haloperoxidase-like catalytic activities of V_2O_5 NWs. NWs were added to a solution containing PR, Br^-, and H_2O_2 to catalyze the production of HOBr, which then reacted with PR to Br_4PR. In this cascade reaction, HOBr generation is the rate-limiting step.[7,8] The following stock solutions were prepared in milliQ water: 1 mM PR, 1 M KBr, 100 mM H_2O_2 (prepared fresh), and 1 mg mL^{-1} V_2O_5 nanowires. The nanowire solution was sonicated for >2 hours before use. The reaction mixture contained these components at the following final concentrations: 50 μM PR, 100 mM Br^-, 5 mM H_2O_2, 0.04 mg mL^{-1} V_2O_5 NWs, 0.5× PBS buffer, and milliQ water to fill the remaining volume. NWs were added to the mixture last to trigger the reaction. For [NW-24 h + TMT3] and [NW-2 h + TMT3], 0.67 μM free TMT3 peptide was also added to the mixture. For measurement with BHI and suppBHI media, milliQ water was completely replaced by the media while the rest of the reactants and buffer concentration remained the same; the final concentration of the media was ~26% v/v.

The bromination of PR (max. absorbance at 430 nm) to Br_4PR (max. absorbance at 590 nm) was measured using an UV-vis spectrophotometer for 10 minutes at 37 °C. The initial rate (v_0) of the bromination reaction was quantified based on the change of Br_4PR concentration, $[Br_4PR]$, over time (eqn (1)), where $[Br_4PR]$ was calculated from absorbance readings using the Lambert–Beer equation (eqn (2)), and the extinction coefficient at 590 nm, ε_{Br_4PR}, used was 72 200 M^{-1} cm^{-1}, as in a previous report.[7]

$$v_0 = \frac{d[Br_4PR]}{dt} \quad (1)$$

$$[Br_4PR] = \frac{A_{590}}{d \times \varepsilon_{Br_4PR}} \quad (2)$$

Antimicrobial assay

S. pneumoniae was first grown on a blood agar (tryptone soy agar with 5% sheep blood, Thermo Scientific) for 15 hours at 37 °C with 5% CO_2. Five to ten colonies from the agar plate was then cultured in 2 mL of a medium (suppBHI) at 37 °C with 5% CO_2 until grown to the mid-log phase. The suppBHI medium consisted of brain heart infusion (BHI) broth (BD bio-

sciences, Becton, NJ, USA) supplemented with 3% horse blood (Hardy Diagnostics, Springboro, OH, USA) and 10 μg mL^{-1} NADH (Millipore, Burlington, MA, USA). For the antimicrobial testing, the bacteria were subcultured into 2 mL of fresh suppBHI and treated with 0.04 mg mL^{-1} nanowires and/or 1 mM KBr. For [NW-24 h + TMT3] and [NW-2 h + TMT3], 0.67 μM free TMT3 peptide was also added to the mixture. The [KBr] group was cultured in suppBHI media and additionally received 1 mM KBr, the [TMT3] group received 0.67 μM free TMT3 and the [Control] group received no nanowire and no KBr. After 15 hours of culture at 37 °C with 5% CO_2, the bacteria cultures were measured for OD600 reading and subsequently, 10 μl of each culture was plated twice onto blood agars for 15 hours at 37 °C with 5% CO_2 for a confirmation reading. For the concentration-dependent kill curve, *S. pneumoniae* was subcultured from the mid-log phase into 2 mL of suppBHI and treated with various concentrations of nanowires and/or 1 mM KBr, then cultured for 15 hours at 37 °C with 5% CO_2 for OD600 reading.

Cytotoxicity assay

The hFB cells (PCS-201-012 from ATCC, Manassas, Virginia, USA) were maintained in Fibroblast Basal Medium (ATCC PCS-201-020) supplemented with Fibroblast Growth Kit – Low Serum (ATCC PCS-201-041) and 1% penicillin/streptomycin (Gibco, Thermo Fisher) and the PC-12 cells in F-12K medium (ATCC) supplemented with 2.5% fetal bovine serum (Gibco), 15% horse serum (Gibco) and 1% penicillin/streptomycin (Gibco). Both cells were cultured in an incubator at 37 °C with 5% CO_2. For cytotoxicity testing, the hFB and PC12 cells were seeded onto 96 well plates at an initial density of 5000 cells per well and cultured for 1 day with 200 μl media per well. Then the nanowires were introduced into the cells by replacing half of the cell culture media with fresh media containing 2× formulations, to make a final concentration of 0.01 mg mL^{-1} or 0.04 mg mL^{-1} nanowires, 1 mM KBr, and 10 μM H_2O_2 in each well. For [NW-24 h + TMT3] and [NW-2 h + TMT3], 0.67 μM free TMT3 peptide was also added to the mixture. Cells were incubated for 24 hours before further analysis. For fluorescent imaging, cells were washed with PBS once and stained with the LIVE/DEAD™ Viability/Cytotoxicity Kit (L3224 from Invitrogen, Thermo Fisher). Live and dead cells were labeled with calcein-AM (1 mM) and ethidium homodimer-1 (2 mM) in PBS, respectively, and incubated at 37 °C for 30 min. Images were captured using a Zeiss LSM 710 confocal microscope and cell viability count was calculated as live cells/ (live cells + dead cells) × 100%. For spectrophotometry reading, cells were treated with the CCK8 mixture from the CCK8/WST-8 Cell Proliferation kit (Cayman Chemical, Ann Arbor, Michigan) for 2 hours at 37 °C and then measured for absorbance at 450 nm. Viability was calculated as

$$(A_{450}^{sample} - A_{450}^{baseline})/(A_{450}^{control} - A_{450}^{baseline}),$$

where $A_{450}^{baseline}$ is the absorbance at 450 nm measured for wells containing only cell media and was incubated for the same amount of time.

Biocompatibility study and *ex vivo* permeation study

All animal experiments were conducted under protocols approved by the Institutional Animal Care and Use Committee (IACUC), in conjunction with the Cornell University's Center of Animal Resources and Education (CARE) Animal Use Guidelines. Healthy adult chinchillas, weight 500–650 g, were obtained from Kuby's Kritters (Akron, NY, USA). For *ex vivo* permeation study, animals were infected with 200 colony-forming unit (CFU) of non-typeable *Haemophilus influenzae* (NTHi) through an intra-bulla injection, which does not hamper the integrity of the tympanic membrane. NTHi was used to induce the middle ear inflammation because it is less virulent than *S. pneumoniae* and less likely to cause severe systemic infections in animals.[39] After 2 days of infection, the animals were euthanized, and the bullae were retrieved. The middle ear chamber side of the bullae was carefully dissected open so that it can be exposed to PBS buffer after the bullae were vertically placed in a 6-well chamber, filled with 8 mL PBS buffer. Tissue integrity was checked using impedance measurement, according to a previous protocol.[7] Selected bullae were then treated with 0.6 mg nanowires, 120 µg (75 mM) KBr, and for the [NW-24 h + TMT3] and [NW-2 h + TMT3] group, 50 µM of free TMT3 peptides in 200 µl PBS. The bullae were incubated at 37 °C and the PBS buffer in the reservoir was collected at the end of the 48-hour release study. For ICP-MS analysis 150 µl of each sample was digested in 600 µl of 25% tetramethylammonium hydroxide (TMAH) and heated at 80 °C for 24 hours. The digested sample was then diluted 50× in 2% nitric acid and filtered with a 0.22 µm filter. Experiments were performed on an Agilent 7800 ICP-MS machine to measure the V-51 isotope and the Br-79 isotope. Total bromide content was calculated as double the Br-79 content, assuming a 50% abundance of the Br-79 isotope. For the biocompatibility study, healthy chinchillas were treated with 0.6 mg nanowires and 120 µg KBr (75 mM) in 200 µl PBS through a non-invasive injection to the outer ear canal using a soft-tipped catheter. The injection was performed under an otoscope connected to a digital camera. After the injection, foam ear plugs were placed into the outer ear canal to prevent formulation leaking. The animals were euthanized after 7 days and the bullae were excised, fixed in 10% formalin, dehydrated and embedded in paraffin for sectioning and H&E staining.

Conclusions

In summary, it has been shown that the synthesis condition of V_2O_5 nanowires could be tuned to produce nanowires with variable sub-micron lengths. Moreover, APTES-functionalized nanowires could be successfully conjugated with a peptide that facilitates trans-tympanic diffusion of therapeutics, *i.e.*, TMT3, onto the surface using the EDC/NHS reaction. The peptide-conjugated nanowires preserved the haloperoxidase-like catalytic activities of V_2O_5 nanowires and demonstrated *in vitro* antimicrobial activity against a H_2O_2-producing bacterium, *S. pneumoniae*, which is a common pathogen of otitis media. Furthermore, the peptide-conjugated nanowires showed improved tissue penetration, compared to unmodified nanowires, across *ex vivo* tympanic membranes from infected chinchillas. For nanowires with smaller profiles, simple mixing with TMT3 peptide also enhanced their *ex vivo* tympanic membrane permeation. These experiments thus demonstrate a potential strategy towards the non-invasive delivery of nanozyme-based antimicrobials for the treatment of otitis media.

Author contributions

S. S. L.: conceptualization, methodology, investigation, visualization, writing – original draft, writing – review & editing; J. L.: conceptualization, methodology; S. W.: investigation, validation, visualization; P. C.: investigation; H. S.: investigation; S. S.: investigation; W. T.: writing – review & editing; X. M.: writing – review & editing; M. D. S.: methodology; R. Y.: supervision, conceptualization, methodology, writing – review & editing, funding acquisition.

Data availability

The data supporting this article have been included as part of the ESI.†

Conflicts of interest

The authors declare no conflict of interest.

Acknowledgements

References

1 S. Tong, C. Amand, A. Kieffer and M. H. Kyaw, *BMC Health Serv. Res.*, 2018, **18**, 318.

2 D. W. Teele, J. O. Klein and B. Rosner, *J. Infect. Dis.*, 1989, **160**, 83–94.

3 M. M. Rovers, A. G. Schilder, G. A. Zielhuis and R. M. Rosenfeld, *Lancet*, 2004, **363**, 465–473.

4 M. Axelsson, *BMC Psychol.*, 2013, **1**, 24.

5 B. Zielnik-Jurkiewicz and A. Bielicka, *Int. J. Pediatr. Otorhinolaryngol.*, 2015, **79**, 2129–2133.

6 R. M. Anderson, *Nat. Med.*, 1999, **5**, 147–149.

7 J. Lang, X. Ma, S. S. Liu, D. L. Streever, M. D. Serota, T. Franklin, E. R. Loew and R. Yang, *Nano Today*, 2022, **47**, 101672.

8 C. D. Pericone, S. Park, J. A. Imlay and J. N. Weiser, *J. Bacteriol.*, 2003, **185**, 6815–6825.

9 A. C. Carr, J. J. van den Berg and C. C. Winterbourn, *Biochim. Biophys. Acta*, 1998, **1392**, 254–264.

10 W. F. McCoy, E. Allain, A. W. Dallmier and S. Yang, Strategies Used in Nature for Microbial Fouling Control: Applications for Industrial Water Treatment, Paper presented at the CORROSION 98, San Diego, California, 1998.

11 Z. Zhang, X. Li, W. Zhang and D. S. Kohane, *Adv. Funct. Mater.*, 2020, 2008701, DOI: 10.1002/adfm.202008701.

12 S. J. Lim, *Acta Otorhinolaryngol. Belg.*, 1995, **49**, 101–115.

13 J. D. Bos and M. M. Meinardi, *Exp. Dermatol.*, 2000, **9**, 165–169.

14 M. R. Prausnitz and R. Langer, *Nat. Biotechnol.*, 2008, **26**, 1261–1268.

15 A. Kogan and N. Garti, *Adv. Colloid Interface Sci.*, 2006, **123–126**, 369–385.

16 L. Sercombe, T. Veerati, F. Moheimani, S. Y. Wu, A. K. Sood and S. Hua, *Front. Pharmacol.*, 2015, **6**, 286.

17 A. Kurabi, K. K. Pak, M. Bernhardt, A. Baird and A. F. Ryan, *Sci. Rep.*, 2016, **6**, 22663.

18 A. Kurabi, D. Schaerer, V. Noack, M. Bernhardt, K. Pak, T. Alexander, J. Husseman, Q. Nguyen, J. P. Harris and A. F. Ryan, *Sci. Rep.*, 2018, **8**, 11815.

19 A. Kurabi, D. Schaerer, L. Chang, K. Pak and A. F. Ryan, *J. Drug Targeting*, 2018, **26**, 127–134.

20 R. André, F. Natálio, M. Humanes, J. Leppin, K. Heinze, R. Wever, H. C. Schröder, W. E. G. Müller and W. Tremel, *Adv. Funct. Mater.*, 2011, **21**, 501–509.

21 P. Hu, P. Hu, T. D. Vu, M. Li, S. Wang, Y. Ke, X. Zeng, L. Mai and Y. Long, *Chem. Rev.*, 2023, **123**, 4353–4415.

22 J. Livage, *Materials*, 2010, **3**, 4175–4195.

23 F. Natalio, R. André, A. F. Hartog, B. Stoll, K. P. Jochum, R. Wever and W. Tremel, *Nat. Nanotechnol.*, 2012, **7**, 530–535.

24 J. Pan, M. Li, Y. Y. Luo, H. Wu, L. Zhong, Q. Wang and G. H. Li, *Appl. Surf. Sci.*, 2015, **333**, 34–38.

25 N. Asim, S. Radiman, M. A. Yarmo and M. S. Banaye Golriz, *Microporous Mesoporous Mater.*, 2009, **120**, 397–401.

26 A.-M. Cao, J.-S. Hu, H.-P. Liang and L.-J. Wan, *Angew. Chem., Int. Ed.*, 2005, **44**, 4391–4395.

27 A. Kurabi, K. Pak, E. Chavez, J. Doan and A. F. Ryan, *Sci. Rep.*, 2022, **12**, 984.

28 S. K. Vashist, *Diagnostics*, 2012, **2**, 23–33.

29 M. Hijazi, V. Stambouli, M. Rieu, V. Barnier, G. Tournier, T. Demes, J.-P. Viricelle and C. Pijolat, *J. Mater. Sci.*, 2018, **53**, 727–738.

30 H. Min, P.-L. Girard-Lauriault, T. Gross, A. Lippitz, P. Dietrich and W. E. S. Unger, *Anal. Bioanal. Chem.*, 2012, **403**, 613–623.

31 R. A. Shircliff, P. Stradins, H. Moutinho, J. Fennell, M. L. Ghirardi, S. W. Cowley, H. M. Branz and I. T. Martin, *Langmuir*, 2013, **29**, 4057–4067.

32 N. Majoul, S. Aouida and B. Bessaïs, *Appl. Surf. Sci.*, 2015, **331**, 388–391.

33 K. H. Sizeland, K. A. Hofman, I. C. Hallett, D. E. Martin, J. Potgieter, N. M. Kirby, A. Hawley, S. T. Mudie, T. M. Ryan, R. G. Haverkamp and M. H. Cumming, *Materialia*, 2018, **3**, 90–96.

34 Z. S. Silva Junior, S. B. Botta, P. A. Ana, C. M. Franca, K. P. Fernandes, R. A. Mesquita-Ferrari, A. Deana and S. K. Bussadori, *Sci. Rep.*, 2015, **5**, 11448.

35 D. Surya Bhaskaram, R. Cheruku and G. Govindaraj, *J. Mater. Sci.: Mater. Electron.*, 2016, **27**, 10855–10863.

36 IARC, Cobalt in Hard Metals and Cobalt Sulfate, Gallium Arsenide, Indium Phosphide and Vanadium Pentoxide, in *IARC Monographs on the Evaluation of Carcinogenic Risks to Humans*, IARC, 2006, vol. 86, https://www.ncbi.nlm.nih.gov/books/NBK321688.

37 J. D. Miller, *J. Acoust. Soc. Am.*, 1970, **48**, 513–523.

38 P. A. Vrettakos, S. P. Dear and J. C. Saunders, *Am. J. Otolaryngol.*, 1988, **9**, 58–67.

39 M. L. Forbes, E. Horsey, N. L. Hiller, F. J. Buchinsky, J. D. Hayes, J. M. Compliment, T. Hillman, S. Ezzo, K. Shen, R. Keefe, K. Barbadora, J. C. Post, F. Z. Hu and G. D. Ehrlich, *PLoS One*, 2008, **3**, e1969.